Journal of Molecular and Cellular Cardiology 150 (2021) 91–100

Contents lists available at ScienceDirect

Journal of Molecular and Cellular Cardiology

journal homepage: www.elsevier.com/locate/yjmcc

Combined high-throughput library screening and next generation RNA sequencing uncover microRNAs controlling human cardiac fibroblast biology

Katharina Schimmel [a], Stevan D. Stojanović [a], Cheng-Kai Huang [a], Mira Jung [a], Martin H. Meyer [a], Ke Xiao [a], Lea Grote-Levi [a], Christian Bär [a], Angelika Pfanne [a], Saskia Mitzka [a], Annette Just [a], Robert Geffers [b], Katharina Bock [a], Franziska Kenneweg [a], Felix Kleemiß [a], Christine S. Falk [c,d], Jan Fiedler [a,*], Thomas Thum [a,e,*]

[a] Institute of Molecular and Translational Therapeutic Strategies (IMTTS), Hannover Medical School, Hannover, Germany
[b] Helmholtz Centre for Infection Research, Research Group Genome Analytics, Braunschweig, Germany
[c] Transplant Immunology, Integrated Research and Treatment Centre Transplantation, Hannover Medical School, Hannover, Germany
[d] German Center for Infection Research (DZIF), Germany
[e] REBIRTH Excellence Cluster, Hannover Medical School, Hannover, Germany

ARTICLE INFO

Keywords:
MiR-20a-5p
miR-132
Novel miRs
Cardiac fibrosis
Autophagy
Reactive oxygen species

ABSTRACT

Background: Myocardial fibrosis is a hallmark of the failing heart, contributing to the most common causes of deaths worldwide. Several microRNAs (miRNAs, miRs) controlling cardiac fibrosis were identified in recent years; however, a more global approach to identify miRNAs involved in fibrosis is missing.
Methods and results: Functional miRNA mimic library screens were applied in human cardiac fibroblasts (HCFs) to identify annotated miRNAs inducing proliferation. In parallel, miRNA deep sequencing was performed after subjecting HCFs to proliferating and resting stimuli, additionally enabling discovery of novel miRNAs. In-depth *in vitro* analysis confirmed the pro-fibrotic nature of selected, highly conserved miRNAs miR-20a-5p and miR-132-3p. To determine downstream cellular pathways and their role in the fibrotic response, targets of the annotated miRNA candidates were modulated by synthetic siRNA. We here provide evidence that repression of autophagy and detoxification of reactive oxygen species by miR-20a-5p and miR-132-3p explain some of their pro-fibrotic nature on a mechanistic level.
Conclusion: We here identified both miR-20a-5p and miR-132-3p as crucial regulators of fibrotic pathways in an *in vitro* model of human cardiac fibroblast biology.

1. Introduction

Heart failure (HF) represents one of the leading causes of deaths worldwide. Moreover, the steady increase of an aging population is expected to further increase the prevalence of HF in the near future. A major pathological hallmark of the failing heart is fibrosis, both in diastolic and systolic HF. Excessive accumulation of collagens leads to progressing stiffness of the heart and consequently, to the reduction of its pump function [1]. Due to persistence of fibrosis even upon conventional therapeutic treatment [2], development of novel therapies targeting fibrosis is expected to substantially improve organ function.

Thus, we here combined a microRNA (miRNA, miR) mimic library screen and an unbiased small RNA deep sequencing approach in primary human cardiac fibroblasts (HCFs) to identify unknown miR candidates driving fibroblast biology as potential targets for anti-fibrotic therapeutics. miRs are small non-coding RNAs that post-transcriptionally

Abbreviations: RNA, Ribonucleic Acid; MiR/MiRNA, MicroRNA; HCF, human cardiac fibroblast; HF, heart failure; ROS, reactive oxygen species; pre-miR, precursor-miR; COL1A1, alpha-1 type I collagen; CTGF, connective tissue growth factor; FOXO3a, Forkhead-Box-Protein O3; LNA, Locked Nucleic Acid; ATG7, Ubiquitin-like modifier-activating enzyme; SOD2, Superoxide dismutase 2; AGO2, Argonaute 2 protein; IL-8, interleukin 8; pri-miR, primary-miR; BLASTN, nucleotide basic local alignment search tool.

* Corresponding authors.
E-mail address: Thum.Thomas@mh-hannover.de (T. Thum).

https://doi.org/10.1016/j.yjmcc.2020.10.008
Received 27 August 2020; Received in revised form 8 October 2020; Accepted 16 October 2020
Available online 28 October 2020

fine-tune gene expression either by AGO2-mediated cleavage or translational repression of their target mRNAs [3]. We show that proliferating conditions induce the expression of the herein identified miRs, miR-132-3p and miR-20a-5p. In the heart, miR-132-3p regulates both hypertrophy and autophagy in cardiomyocytes [4]. Therapeutic miR-132-3p inhibition in small and large animal models of myocardial ischemia improves cardiac remodelling and function [5]. Synthetic miR-20a-5p blockade prevents right ventricular hypertrophy in a mouse model of pulmonary hypertension [6]. Here, we provide evidence that miR-132-3p and miR-20a-5p repress fibroblast autophagy and detoxification of reactive oxygen species (ROS) in HCFs, thereby regulating crucial cellular pathways in cardiac fibroblasts that may impact on miR-based therapeutic outcome.

2. Results

2.1. MiR mimic library screen and miR deep sequencing identify pro-fibrotic miR-132-3p and miR-20a-5p in HCFs

MiRs are involved in fibrosis-development caused by pressure overload or cardiac transplantation in rodents [7,8]; however, their functional significance in activation or repression of fibrotic pathways in cardiac fibroblasts in the human system is still not well understood. Therefore, we performed a miR mimic library screen consisting of 2555 human mature miRs (100% coverage of miRBase Sequence Database Version 20) in HCFs to identify pro-proliferative miRs that could be potentially targeted using antisense-chemistries. The rationale of screening for proliferation activity of HCFs is strongly strengthened by

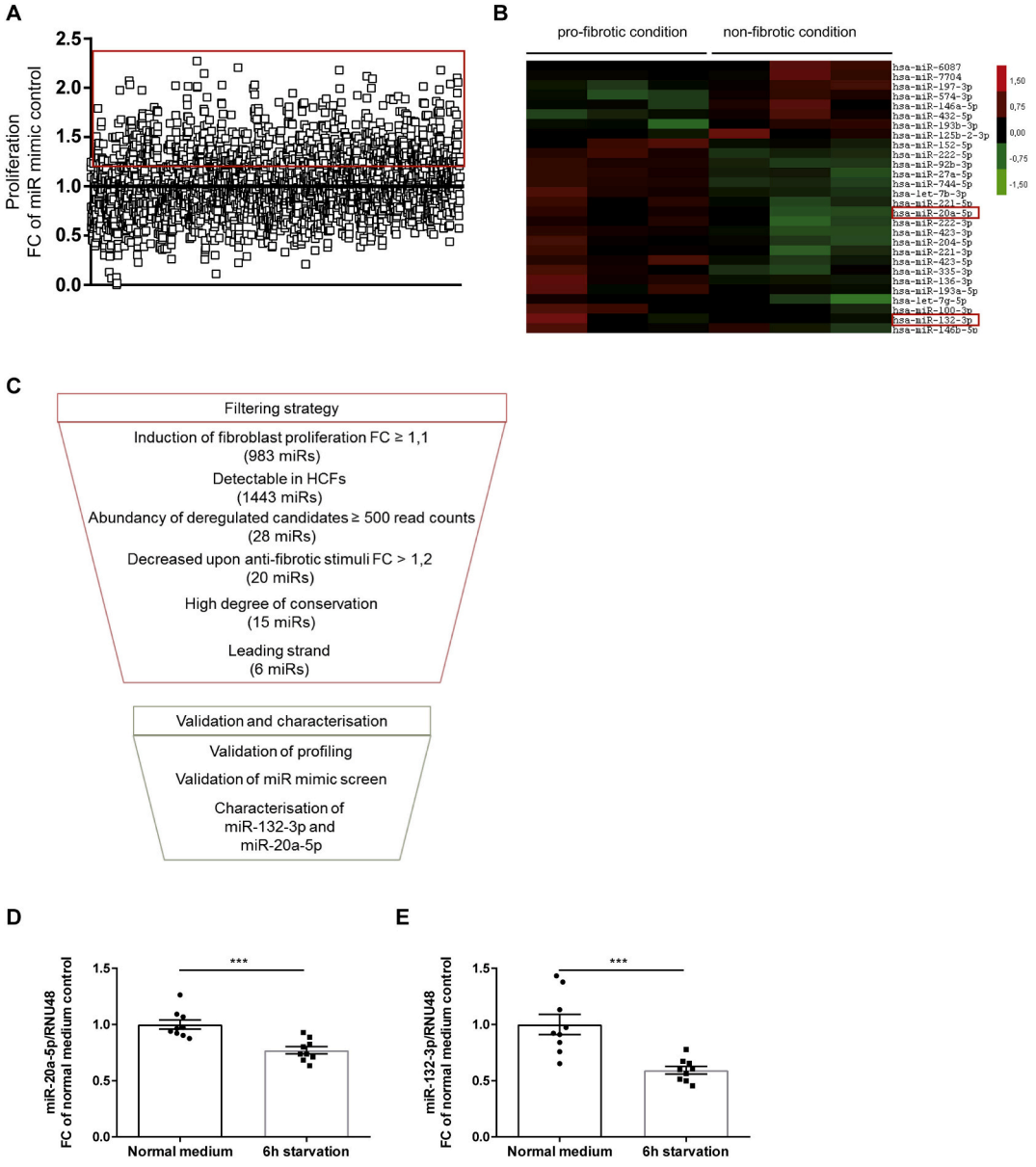

Fig. 1. MiR mimic library screen and miR deep sequencing identify annotated pro-fibrotic miR candidates in HCFs. (A) Functional screen of specific 2555 miR mimics overexpressed in HCFs. The cells were transfected with 30 nM miRVana miR mimics 48 h before proliferation of HCFs was measured by BrdU-ELISA. 983 candidates enhancing fibroblast proliferation FC $\geq$ 1.1 are highlighted by red rectangle. (B) Differentially expressed miRs in HCFs grown under standard medium condition (10% FCS) relative to HCFs cultivated in starvation medium (0.1% FCS) for 6 h ($n = 3$). Lead candidates miR-132-3p and miR-20a-5p are highlighted by red rectangle. (C) Strategy of filtering, validation and characterisation of miR candidates leading to the identification of miR-132-3p and miR-20a-5p. (D, E) Decreased levels of miR-132-3p and miR-20a-5p in HCFs cultivated in starvation medium (0.1% FCS) for 6 h, confirmed by quantitative real-time PCR (unpaired *t*-test, $n = 9$). *** $p \leq 0.001$. (For interpretation of the references to color in this figure legend, the reader is referred to the web version of this article.)

the study of Moore-Morris et al. convincingly demonstrating that fibroblast accumulation is mainly attributed to proliferation of tissue-resident fibroblast populations upon pressure-overloaded conditions [9]. Applying a selection threshold of augmentation of fibroblast proliferation FC (fold change) ≥ 1.1; we identified 983 miR candidates that increased HCF proliferation upon overexpression (Fig. 1A).

In parallel, miR deep sequencing was performed comparing dysregulated miRs in HCFs upon proliferating conditions compared to resting conditions *in vitro* (Fig. 1B). Next, we focused on selecting meaningful miR-candidates by applying stringent refining criteria as shown in Fig. 1C: First, we filtered out low abundant miRs (less than 500 average read counts in all samples) of the total 1443 candidates detectable in HCFs. Out of the remaining 28 candidates, levels of 20 miRs were found being decreased (absolute fold change >1.2) following anti-fibrotic, resting stimuli in HCFs (confirmed by quantitative real-time PCR as indicated for the two lead candidates in Fig. 1D & E) and therefore are potential regulators of fibroblast turnover. Out of these miRs, 15 candidates were conserved in mouse (100% sequence identity according to miRBase Sequence Database Version 21) and 6 out of them represented the leading strand. Lastly, we combined this final dataset with miRs found in the initial screen, increasing fibroblast proliferation FC $\geq$ 1,1 upon miR enhancement (Fig. 1A). By this strategy, we identified particularly miR-132-3p to promote fibroblast proliferation (Supplementary Fig. 1A). Moreover, HCFs migrated substantially faster upon overexpression of miR-132-3p or miR-20a-5p as evidenced by a scratch wound assay (Fig. 2A & B). Furthermore, HCFs transfected with precursor-(pre-)miR-132 or mature miR-20a-5p mimic showed increased mRNA-levels of the extracellular matrix (ECM) proteins, the fibrosis markers, *alpha-1 type I collagen (COL1A1)* and *connective tissue growth factor (CTGF)*, respectively, as indicators of a pathologically "active" state (Fig. 2C & D). Importantly, endogenous upregulation of the two investigated miRs correlated with higher COL1A1- and CTGF-protein expression, respectively, in HCFs (Fig. 2E & F). Taken together, in-depth *in vitro* studies indicate that miR-132-3p and miR-20a-5p are sufficient to drive a complex set of fibrotic responses in HCFs.

2.2. MiR-132-3p and miR-20a-5p target key players of autophagy and detoxification of reactive oxygen species in HCFs

We next aimed to study the molecular functions of miR-132-3p and miR-20a-5p in the regulation of cardiac fibrosis in the human system. Interestingly, bioinformatic target-analysis using TargetScanHuman (Version 7.1) [3], predicted key players of pathways important for cellular homeostasis, namely autophagy and detoxification of ROS, as putative target genes.

We have previously shown that miR-132-3p directly targets the pro-autophagic transcription factor FOXO3a in rodent cardiomyocytes, hereby augmenting hypertrophy [4]. Here, we validated FOXO3a as target of miR-132-3p in HCFs and explored its functional role in cardiac fibroblasts *in vitro*. In line, transfection of HCFs with pre-miR-132 led to repression of FOXO3a as evidenced on translational level (Fig. 3A) but not on transcriptional level (Supplementary Fig. 1C). Conversely, de-repression of FOXO3a occurred upon inhibition of the miR using locked nucleic acid (LNAs) oligonucleotides complementary to the sequence of miR-132-3p (Fig. 3B), but again not on transcriptional level (Supplementary Fig. 1D). 3′ untranslated regions (3′UTR) of Ubiquitin-like modifier-activating enzyme ATG7, a protein essential for autophagy, and Superoxide dismutase 2 (SOD2), both harbour sites complementary to the seed region of miR-20a-5p (Fig. 3C). To validate this bioinformatics prediction, we cloned the 3′ UTR of *ATG7* and *SOD2* downstream of the firefly luciferase gene and confirmed a significantly reduced normalized luciferase activity upon co-transfection of both constructs with miR-20a-5p mimics compared to the control (Fig. 3D & E). These results confirm direct interaction of miR-20a-5p with predicted target sites in the 3′UTR of *ATG7* and *SOD*. Whereas protein levels of *ATG7* did not change upon overexpression of miR-20a-5p (Supplementary Fig. 1D), a significant de-repression of ATG7 protein was observed upon miR-20a-5p inhibition in HCFs, respectively (Fig. 4A). In contrast, targeting of SOD2 by miR-20a-5p was evident both on transcriptional as well as translational level in HCFs (Fig. 4B & C), pointing towards an mRNA-cleavage mediated repression of this target. In line, endogenous miR-20a-5p repression *via* LNA technology enhanced SOD2 expression mildly (Fig. 4D).

Taken together, the two identified fibroblast miRs repressed important components of autophagy and detoxification of reactive oxygen species in HCFs, suggesting a possible functional role of these downstream pathways in counteracting the fibrotic phenotype.

2.3. MiR-132-3p and miR-20a-5p regulate autophagy and detoxification of ROS in HCFs

Our results suggest a possible involvement of repressed autophagy and antioxidant system in the miR-132-3p and miR-20a-5p mediated fibrotic response, thus we decided to further study the role of these pathways in HCF biology. To determine whether activation of COL1A1 upon overexpression of miR-132 (Fig. 1E & F) might be attributed to its repression of the pro-autophagic transcription factor FOXO3a (Fig. 3A), COL1A1 levels were monitored in HCFs upon silencing of *FOXO3a* (Fig. 5A). Indeed, transfection of HCFs with siRNA *FOXO3a* prominently augmented COL1A1 production, suggesting an anti-fibrotic role of FOXO3a (Fig. 5B & C). Consistently, our own results showed a potential correlation of a diminished fibrotic phenotype of HCFs with autophagy, stimulated by the chosen model of 6 h starvation period (Fig. 5D**,** Supplementary Fig. 2B & C), a caloric restriction mimetic (Quercetin) or an mTOR-inhibitor (Torin1) (Supplementary Fig. 2D & E). However, detection of selected fibrotic markers at protein level only highlighted mild repressive effects, suggesting later time points of interest, too. To explore whether miR-132 might functionally impact on the autophagic processes in HCFs, we overexpressed miR-132 and found a decreased mean fluorescence signal of a dye specifically staining autophagic compartments (Supplementary Fig. 3A). Importantly, this decline was evident both under basal conditions and after treatment of HCFs with the lysosomal inhibitor chloroquine, which blocks autophagosome turnover, hereby enabling monitoring of the autophagic flux. In addition, specific silencing of *ATG7*, a protein essential for autophagy, strongly augmented secretion of the pro-inflammatory cytokine IL-8 by HCFs thereby controlling fibroblast turnover (Supplementary Fig. 3B) whereas short-term starvation repressed IL-8 secretion *in vitro* (Fig. 5E). These results support both anti-fibrotic and anti-inflammatory roles of the autophagic pathway in HCFs. Repression of autophagy *via* the molecular targets FOXO3a and ATG7 by miR-132-3p and miR-20a-5p, respectively, possibly explains their pro-fibrotic nature on a mechanistic level.

Based on our results, miR-20a-5p impinges on both defence systems (Fig. 3D & E). Therefore, we followed ROS-production upon overexpression and inhibition of miR-20a-5p as well as silencing of the targets *ATG7* and *SOD2* in HCFs. In line, both miR-20a-5p overexpression and silencing of *SOD2* led to an increase, whereas miR-20a-5p inhibition diminished ROS-production (Supplementary Fig. 3C **and** Supplementary Fig. 3D–E). Intriguingly, silencing of *ATG7* did not show any impact on ROS levels in HCFs (Supplementary Fig. 3C **and** Supplementary Fig. 3F). This study highlights the regulation of ROS *via* miR-20a-5p, which seems to be dependent on repression of the target *SOD2*, but not *ATG7*. Most likely, mitophagy plays a downstream role in the removal of ROS *via* selective degradation of damaged or dysfunctional mitochondria rather than macro-autophagy.

Taken together, our results imply a crucial protective role of cellular homeostasis counteracting fibroblast-activation. A schematic representation of the modulation of these pathways by miR-132-3p and miR-20a-5p and their contribution to the fibrotic phenotype of cardiac fibroblasts is depicted in Fig. 5F.

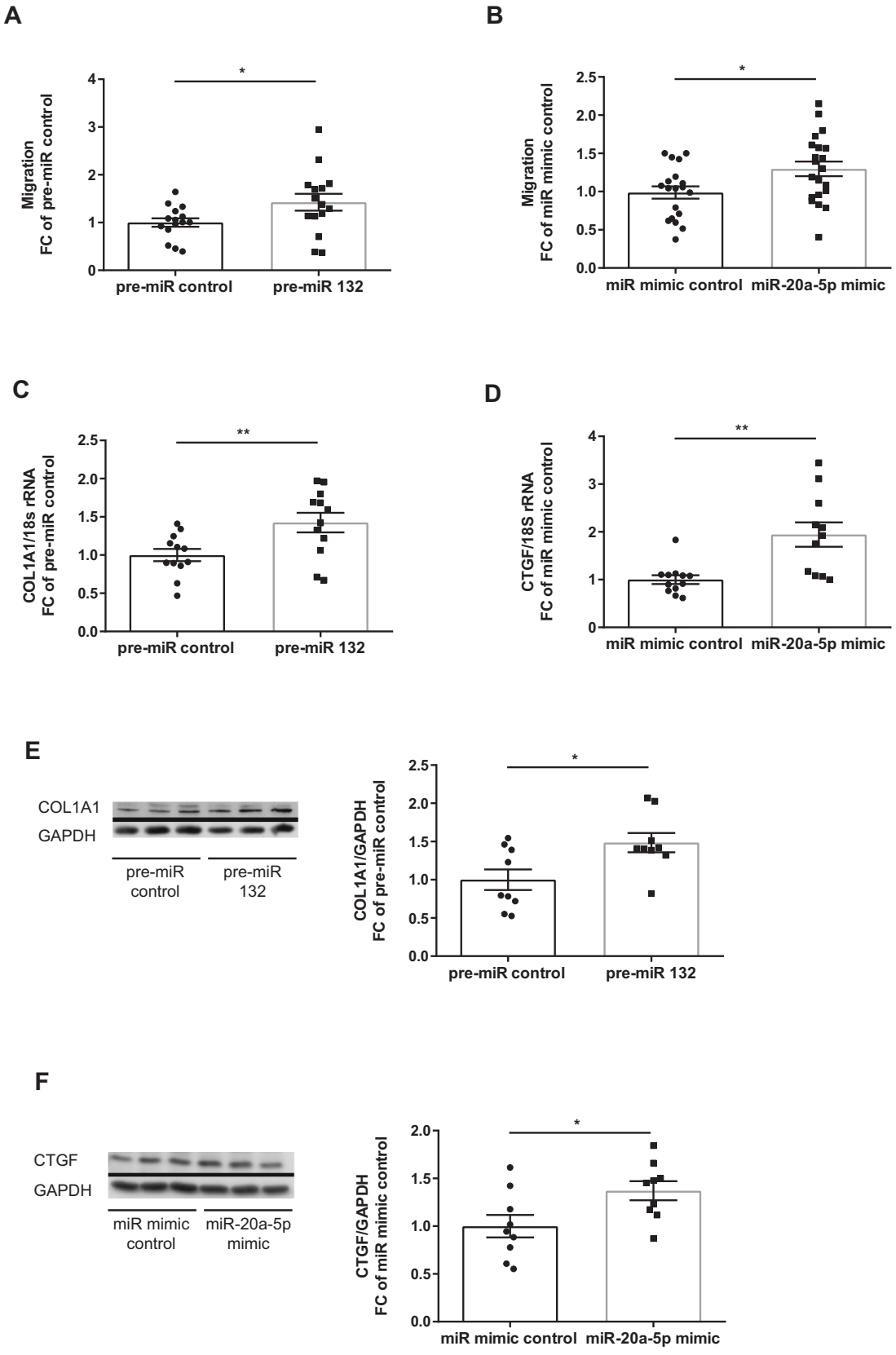

Fig. 2. MiR-132-3p and miR-20a-5p alter human cardiac fibroblast biology.
(A, B) Enhancement of migration activity in primary HCFs after overexpression of miR-132-3p or miR-20a-5p (unpaired *t*-test, $n = 15, 19/21$). (C, D) Significant activation of *COL1A1*- and *CTGF*-transcription in HCFs transfected with pre-miR-132 or miR-20a-5p mimic (unpaired t-test, $n = 12$). (E, F) MiR-132 and miR-20a-5p significantly increase expression levels of COL1A1 and CTGF, respectively, in HCFs as shown in a representative Western Blot (unpaired t-test, $n = 9$). * $p \leq 0.05$, ** $p \leq 0.01$.

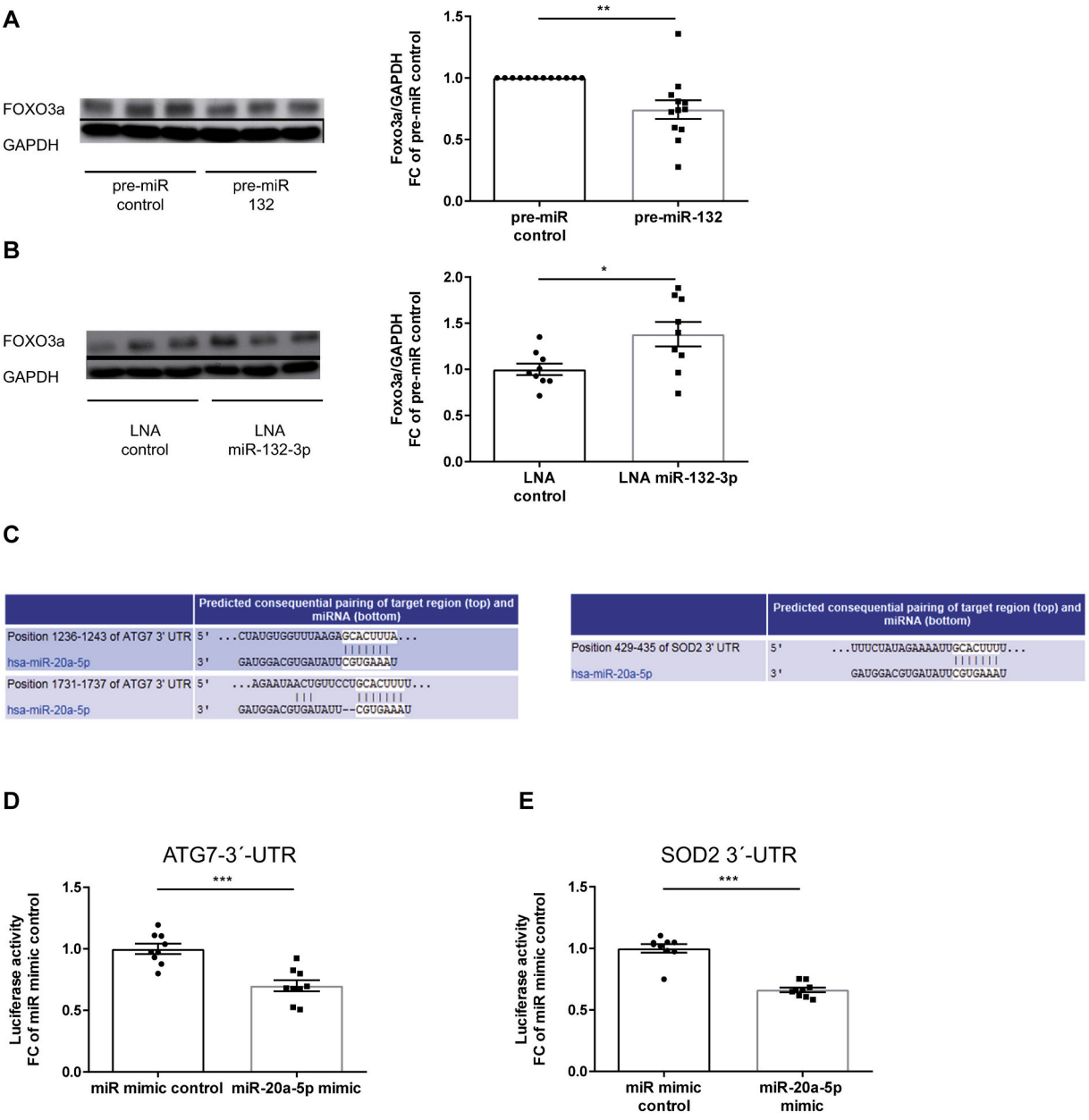

Fig. 3. MiR-132-3p targets FOXO3a and miR-20a-5p targets ATG7 as well as SOD2 in HCFs. (A) Decreased expression of FOXO3a on protein levels in HCFs upon overexpression of miR-132 (unpaired t-test/one-sample t-test, $n = 12$). (B) Increased expression of FOXO3a on protein levels in HCFs upon inhibition of miR-132-3p (unpaired t-test, $n = 9$). (C) Predicted base-pairing between the seed sequence of miR-20a-5p and complementary regions in the 3′ untranslated regions (3'UTR) of *ATG7* and *SOD2* (TargetScanHuman, version 7.1). (D, E) Normalized luciferase activity following co-transfection of a luciferase construct containing the 3′UTR of *ATG7* or *SOD2* with miR mimic control or miR-20a-5p mimic (unpaired t-test, $n = 9$).).* $p \leq 0.05$, ** $p \leq 0.01$, *** $p \leq 0.001$.

3. Discussion

Here, we identified the highly conserved miR-132-3p and miR-20a-5p and unravelled their crucial role in activating the fibrotic program in human cardiac fibroblasts. In line, miR-132 was previously found to be activated in hearts of hypertensive rats and patients [10], suggesting an evolutionary conservation of this upregulation. Likewise, miR-20a-5p levels were prominently increased in sera taken from patients suffering from hepatitis C-induced liver fibrosis [11], however no cardiac fibroblast function was reported so far. In a seminal microRNA study from the Dimmeler lab, endothelial miR-20a was reported to be anti-angiogenic and thus a therapeutic candidate for modulation of endothelial biology [12]. Cardiomyocyte miR-132-3p regulates cardiac hypertrophy by targeting the pro-autophagic transcription factor FOXO3a [4]. Combining these findings with our results on fibroblast biology herein highlights miR-132-3p as the most interesting candidate for therapeutic miRNA modulation. In line, Foinquinos et al. recently demonstrated that targeting of miR-132-3p *in vivo* reduced ischemia-related cardiac fibrosis further supporting our *in vitro* data [5]. These findings highlight general clincial translation of the *in vitro* findings from our combined model approach. Clinical phase I study has been completed for therapeutic miR-132 antagonism (ClinicalTrials.gov Identifier: NCT04045405).

Nevertheless our combined model systems have limitations. First, miRNA overexpression library screening could artificially enhance miRNA expression that is never reached in a physiological setting. Next to this limitation by miRNA biology, we only screened with one well per miRNA, thus technical issues may hamper interpretation of screening data. However, we were able to validate previously reported pro-fibrotic

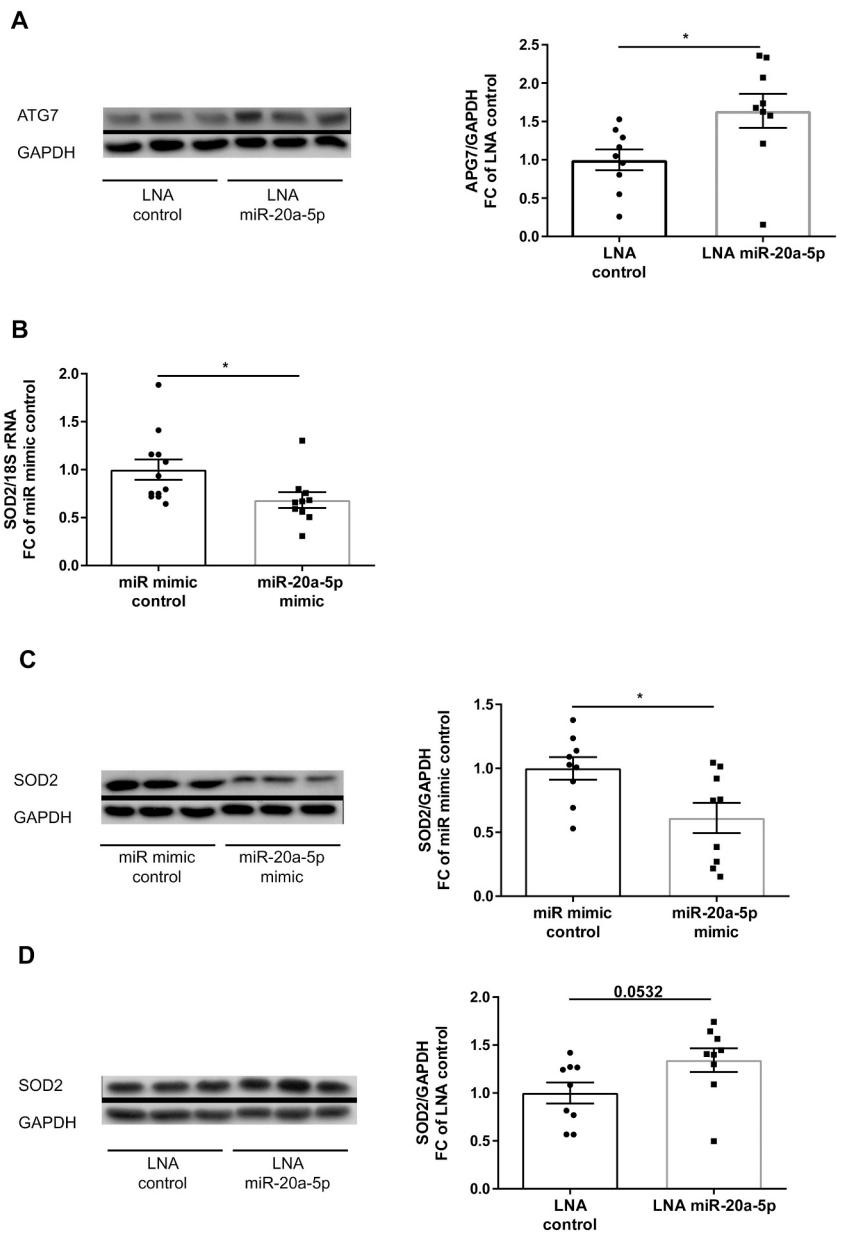

Fig. 4. Modulation of ATG7 *via* miR-20a-5p.
(A) De-repression (A) of APG7 protein upon inhibition of miR-20a-5p in HCFs (unpaired t-test, $n = 9$). Decreased SOD2 mRNA (B) and protein expression (C) in HCFs upon over-expression of miR-20a-5p (unpaired t-test, $n = 12, 9$). De-repression of SOD2 upon inhibition of miR-20a-5p in HCFs appears more evident on protein level (D) (unpaired t-test, $n = 9$).* $p \leq 0.05$.

properties for miR-199 family member hsa-miR-199a-3p [13] and for miR-208 family members hsa-miR-208a-3p and hsa-miR-208b-5p [14]. Second, 2d cell culture of fibroblasts could be very different from any fibroblast behaviour *in vivo*, thus recapitulating findings in 3d systems or organoids could be useful. Third, RNA sequencing only identifies annotated miRNAs, thus novel sequences have to be identified with a different *in silico* approach and could be another task for future studies.

Herein described autophagy is a cellular process of self-renewal and was described as an adaptive and protective response to heart failure in cardiomyocytes [15]. However, the role of autophagy in cardiac fibrosis is widely unknown. Here, we provide evidence for anti-fibrotic and anti-inflammatory functions of autophagy and show upstream post-transcriptional regulation of this pathway by both miR-132-3p and miR-20a-5p. Based on our results, the pro-fibrotic potential of miR-132-3p and miR-20a-5p is most likely attributed to their repressive effects on the pro-autophagic transcription factor FOXO3a and the autophagy-essential protein ATG7 in cardiac fibroblasts, the effector cells of myocardial fibrosis. This result goes in line with the observation made by Aranguiz-Urroz et al. indicating that induction of autophagy leads to enhanced degradation of collagen type I in cardiac fibroblasts *in vitro* [16]. *In silico* approaches such as investigation of ATG7-dependent miRNA expression demonstrated by Stojanovic and colleagues [17], could further add mechanistic insight on downstream cellular impact. The lack of animals with fibroblast-specific autophagy deficiency still hampers analysis of a possible causal contribution of abolished autophagy to myocardial fibrosis *in vivo*.

Oxidative stress is intimately and causally linked to development and persistence of cardiac fibrosis (reviewed in [18]). Endogenous ROS neutralization diminishes myocardial fibrosis and attenuates cardiac dysfunction and aging [19]. The antioxidant system represents the first defensive line with SOD2 being an integer part of ROS-detoxifying enzymes. Here, we provide evidence for miR-20a-5p mediated regulation of ROS accumulation in HCFs. This highlights miR-20a-5p as a putative therapeutic target, particularly in post-cardiac-transplantation medicine. In this setting, both fibrosis and ROS are major determinants for graft failure [20].

In conclusion, we here present miRs driving fibrotic responses by perturbing crucial pathways of cellular homeostasis. These cellular

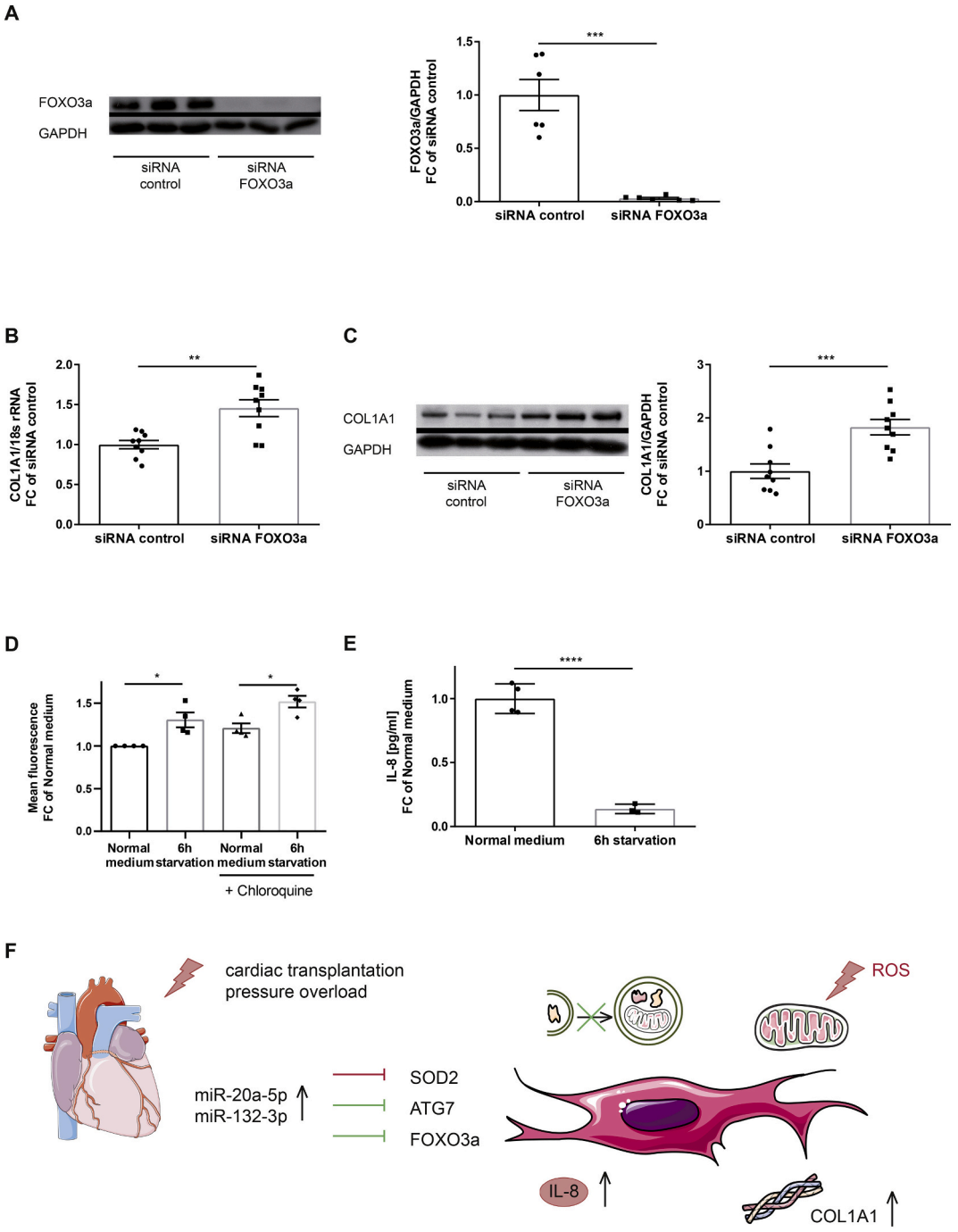

Fig. 5. Autophagy signalling contributes to fibrotic responses of HCFs.
(A) siRNA-mediated silencing of *FOXO3a* leads to decreased FOXO3a protein levels in HCFs (unpaired t-test, $n = 6$). Increased expression of COL1A1 on mRNA (B) and protein levels (C) in HCFs upon silencing of miR-132-3p target *FOXO3a* (unpaired t-test, $n = 9$). (D) Both under basal conditions and after treatment of HCFs with the lysosomal inhibitor chloroquine, fluorescent signal of autophagic compartments increases upon short-time starvation, demonstrating increased autophagic flux in HCFs (one-sample t-test and unpaired t-test, $n = 4$). (E) Diminished release of pro-inflammatory cytokine IL-8 in HCFs grown in starvation medium (0.1% FCS) for 6 h. (F) Schematic representation of the impact of miR-132-3p and miR-20a-5p on cellular pathways of homeostasis and the fibrotic response in HCFs in cardiac disease. * $p \leq 0.05$, ** $p \leq 0.01$, *** $p \leq 0.001$.

pathways are important for cell maintenance both within the heart and other tissue. Therefore, targeted inhibition of especially cardiac miR-132-3p might be safely applied to ameliorate cardiac fibrosis, a major critical factor for the impairment of cardiac performance.

4. Materials and methods

4.1. Cell culture, transfection, and treatment

Human cardiac fibroblasts (HCFs, Promocell) were cultured in fibroblast basal medium FBM-3 supplemented with 10% fetal bovine serum (FCS), supplements (Promocell), 100 µg/ml penicillin and 100 µg/ml streptomycin under standard cell culture conditions (37 °C, 5%

CO 2). Throughout the experiments, HCFs from two – three donors were used in all experiments at passages 5–9. Transfection was carried out using specific miR mimics, pre-miRs, LNAs or negative controls (mirVana® miRNA mimics, Applied Biosystems; pre-miR-132, Ambion; LNA oligonucleotides, Exiqon) at a final concentration of 30 nM. All transfections were performed using Lipofectamine 2000 reagent (Invitrogen) according to the manufacturer's protocol. Cells were analysed in functional assays as indicated and for mRNA 48 h, for protein expression 72 h after liposomal transfection. For short-time starvation experiments, HCFs were kept in FBM-3 supplemented with 0,1% FCS and 100 μg/ml penicillin and 100 μg/ml streptomycin for 6 h. Treatment with chloroquine was performed at 10 μM for 24 h. HEK293 cells were cultured in DMEM supplemented with 10% FCS, 100 μg/ml penicillin and 100 μg/ml streptomycin under standard cell culture conditions (37 °C, 5% CO 2).

4.2. RNA isolation

Total RNA of tissues, fractionated and cultured cardiac cells was isolated using RNeasy Mini Kit (Qiagen) or TriFast method (Peqlab) according to the manufacturer's instructions. Subsequent quantification and quality control was performed with Synergy HT Reader (BioTek).

4.3. qRT-PCR analysis

Prior to quantitative detection of mRNAs, reverse transcription of 100–1000 ng total RNA was performed using the iScript Select cDNA synthesis kit (Bio-Rad), following the manufacturer's instructions. Real-time qPCR was performed in a CFX96 Touch™ Real-Time PCR Detection System (Biorad, Hercules, USA) with specific primers (Supplementary Table 1) and the iQ SYBR Green Mix (Bio-Rad) according to the manufacturer's protocol. 18S ribosomal RNA (18S rRNA) was used as housekeeping control for gene-specific expression levels.

For miRNAs quantification, specific TaqMan MicroRNA Assays (Supplementary Table 1) were used following the manufacturer's protocol using 50 ng total RNA. MiRNAs were quantified using the ViiA™ 7 Real-Time PCR System (Life Technologies, Carlsbad, USA). MiRNA levels were normalized to the small RNA molecule snoRNA-202 for mouse and to RNU48 for human samples (Table 1).

Table 1
qPCR primers and TaqMan miRNA detection assays used in this study.

qPCR primers (mRNA)		
Name	Forward primer (5′- > 3′)	Reverse primer (5′- > 3′)
hsa-18S rRNA	AGTCCCTGCCCTTTGTACACA	GATCCGAGGGCCTCACTAAAC
mmu-18S rRNA	GTAACCCGTTGAACCCCATT	CCATCCAATCGGTAGTAGCG
hsa-GAPDH	CCAGGCGCCCAATACG	CCACATCGCTCAGACACCAT
hsa-SOD2	CAAATTGCTGCTTGTCCAAA	TCTCCCAGTTGATTACATTCCA
hsa-COL1A1	QuantiTect Primer Assay: QT00037793 (Qiagen, Hilden Germany)	
hsa-CTGF	QuantiTect Primer Assay: QT00052898 (Qiagen, Hilden Germany)	
hsa-FOXO3a	QuantiTect Primer Assay: QT00031941 (Qiagen, Hilden Germany)	
hsa-ATG7	QuantiTect Primer Assay: QT00008974 (Qiagen, Hilden Germany)	

TaqMan assays (miRNA)	
Name	
RNU48	TaqMan Assay: 001006 (Applied Biosystems, Foster City, CA, USA)
mmu-snoRNA-202	TaqMan Assay: 001232 (Applied Biosystems, Foster City, CA, USA)
hsa-miR-132	TaqMan Assay: 000457 (Applied Biosystems, Foster City, CA, USA)
hsa-miR-20a	TaqMan Assay: 000580 (Applied Biosystems, Foster City, CA, USA)
Custom TaqMan® Small RNA Assay	TaqMan Assay: Customised (Applied Biosystems, Foster City, CA, USA)

4.4. Protein extraction and Western-Blotting

Cells were lysed using lysis buffer containing protease inhibitor Pefabloc (Sigma). Proteins were separated *via* sodium dodecyl sulfate polyacrylamide gel electrophoresis (SDS-PAGE) and transferred to polyvinylidene difluoride (PVDF) membranes. Subsequently, membranes were blocked with 5% milk in Tris-buffered-saline-Tween (TBS-T). The following primary antibodies were incubated overnight in 5% milk in TBS-T: COL1A1 (Sigma Aldrich, #HPA008405), CTGF (Abcam, #ab6992), FOXO3a (Cell Signalling, #ab2497), SOD2 (Abcam, #ab16956), APG7 (Santa Cruz, # sc-376,212), GAPDH (Abcam, #ab8245). Binding of secondary antibody conjugated with horseradish peroxidase (HRP) was visualized using chemiluminescence, and quantified using ImageJ software.

4.5. Protein multiplex analysis for the quantification of IL-8

The IL-8 levels in the supernatants of cultured HCFs were measured using the Luminex-based multiplex technology (Bio-Plex murine cytokine multiplex assays, Bio-Rad, Hercules, USA) according to the manufacturer's instructions. In brief, culture supernatant was diluted with sample diluent 1:1 and incubated with color-coded beads covered with capture antibodies for IL-8. After 1 h incubation and washing, bead-bound IL-8 was quantified by biotinylated detection antibodies followed by streptavidin-PE staining. Concentrations were measured by parallel standard curves for each parameter and the 5 parameter logistic plots for linear regression based on the MFI of 50–100 beads per cytokine per sample using the Bio-Plex Manager 6.1 software.

4.6. Ago2 pull down experiments

Argonaute pull down was performed using Dynabeads Protein G following the manufacturer's instructions. HCFs were seeded in T150-er flasks and transfected with a customised miR-mimic of the novel miR or miR-mimic control (Ambion) using Lipofectamine 2000. Medium change was done after 4 h and the HCFs were harvested 48 h later. For immunoprecipitation, Dynabeads Protein G (Invitrogen, #100-04D) were incubated with 5 μg of Argonaute 2 antibody (Thermo Pierce #MA5-14861) and control IgG in citrate-phosphate buffer at 4 °C for one hour. HCF cell pellets were lysed in NP40 lysis buffer (Life Technologies) and incubated with bead bound antibody for 2 h at 4 °C. After washing, bead-pellet was used for western blotting or RNA isolation using miRNeasy kit (Qiagen). Equal volume of isolated RNA was reverse transcribed as before and the novel miR was amplified using a customised Taqman assay (Applied Biosystems). Enrichment of the novel miR in comparison to miR-mimic control was evaluated in novel miR-overexpression condition. Normalization was done by using control IgG values.

4.7. MicroRNA target prediction

The microRNA databases and target prediction tools miRBase (http://microrna.sanger.ac.uk/), PicTar (http://pictar.mdc-berlin.de/) and TargetScan (http://www.targetscan.org/index.html) were used to search for potential miR targets.

4.8. Luciferase assay

The 3'UTR sequence of predicted miR targets of interest bearing the respective seed regions were cloned into a pMIR-REPORT vector (Ambion). HEK 293 cells were cotransfected with the cloned constructs, a β-galactosidase control plasmid (Promega) and with pre-miRs of interest or control using Lipofectamine 2000. 20 ng of plasmid and 100 nM of miR was used. 24 h after transfection, luciferase and b-galactosidase activity was measured using the Luciferase Assay System (Promega) and Beta-Galactosidase Assay system (Promega) kits on a multi-plate reader

(Biotek, Synergy HT) according to the manufacturer instructions.

4.9. Proliferation assay

Bromodeoxyuridine (BrdU) Cell Proliferation ELISA Kit (Cell Proliferation ELISA, BrdU, colorimetric, Roche) was used to measure the proliferation rate of HCFs following the manufacturer's instructions.

4.10. Scratch wound assay

The migration of HCFs was evaluated by a scratch assay. A manual scratch was done using the broader side of a 200 µl pipette tip to remove cells in a discrete area of the confluent monolayer. Two representative pictures of each well were captured before the cells were incubated under standard cell culture conditions (37 °C, 5% CO 2) for 6 h. Then, the same areas of the wells were re-captured. Cell-free areas before and after migration were analysed using the Nikon NIS-Elements BR Imaging software.

4.11. AnnexinV-7AAD-staining

For differentiation between viable, apoptotic and necrotic cells FlowColletTM Annexin Red Kit (Millipore) was used to compare HCFs grown under standard normal medium with short-term starvation conditions according to the manufacturer's instructions. The fluorescence intensity for 7-AAD and Annexin-V for each single cell was analysed using guava easyCyteTM Flow Cytometer (Merck-Millipore, Darmstadt, Germany).

4.12. Dihydroethidium staining

HCFs were stained with dihydroethidium (DHE, Invitrogen) to detect intercellular levels of ROS. In brief, cells were harvested and stained with DHE at a final concentration of 5 µM under standard cell culture conditions (37 °C, 5% CO 2) for 30 min. Red fluorescence intensity of oxidized DHE was determined using guava easyCyteTM Flow Cytometer (Merck-Millipore, Darmstadt, Germany).

4.13. CYTO-ID staining

For detection of autophagy, HCFs were stained with CYTO-ID® Green dye (Enzo) according to the manufacturer's instructions. In brief, the cells were incubated with CYTO-ID staining solution (CYTO-ID detection reagent 1:1000 in phenol red-free FBM-3 supplemented with 10% FCS, supplements, 100 µg/ml penicillin and 100 µg/ml streptomycin) under standard cell culture conditions (37 °C, 5% CO 2) for 30 min. Cells were harvested and the mean fluorescence intensity for CYTO-ID® Green of the stained population was assessed using guava easyCyteTM Flow Cytometer (Merck-Millipore, Darmstadt, Germany).

4.14. MicroRNA profiling

Global miR profiling was performed in primary HCFs after they were kept in FBM-3 supplemented with 0,1% FCS and 100 µg/ml penicillin and 100 µg/ml streptomycin for 6 h and standard normal medium control. Total RNA was isolated with the miRNeasy Mini Kit (Qiagen), quantified and quality-assessed by NanoDrop ND-1000 and Agilent Bioanalyzer 2100 (triplicates from 3 independent experiments were pooled per group). Illumina TruSeq® Small was applied to prepare the samples for subsequent deep sequencing on the Genome Analyzer IIx (Illumina Genome Analyzer IIx) platform with a sequencing depth of 5 × 106 reads. Oasis server was used for analysis of raw data and Cluster 3.0 for hierarchical clustering to present deregulated miRs in a heatmap.

4.15. Statistical analysis

In vitro experiments were performed *n*-independent times, as indicated in the figure captions. Data are displayed as mean of independent experiments/independent animal samples ± SEM. Statistical analysis was carried out using the GraphPad Prism 6 software on the whole dataset. For comparison of two groups, unpaired two-tailed Student's *t*-test, and for analysis of three or more groups one-way ANOVA with Bonferroni's multiple comparisons test was applied, unless otherwise stated in the figure legends. A *p*-value of 0.05 or lower was considered statistically significant.

Supplementary data to this article can be found online at https://doi.org/10.1016/j.yjmcc.2020.10.008.

Author contributions

KS, JF & TT together developed the concept and designed this study. KS, MJ, JF and TT wrote the manuscript and together with SDS, CKH, MHM, AP, AJ, LGL, KB, SM, CB, FK and FK performed *in vitro* experiments, Real Time PCR, and Western Blots and analysed the data. JF was involved in FACS and Luciferase experiments. *CF* performed the cytokine multiplex assay, RG the small RNA deep sequencing and KX assisted in the bioinformatics part.

Disclosure

TT filed and licensed patents in the field of noncoding RNAs. TT is founder and holds shares of Cardior Pharmaceuticals GmbH.

Funding

This study was partly funded by the European Union project Fibrotarget (7th Framework Project; to TT), the ERC Consolidator Grant Longheart and the ERANET Grant EXPERT (to TT).

Acknowledgements

We are thankful to the Hannover Biomedical Research School (HBRS), Hannover Medical School, Germany and to the Integrated Research and Treatment Center Transplantation (IFB-Tx), Hannover Medical School, Germany for financial support to LGL and KB.

References

[1] E. Braunwald, Heart failure, JACC Heart Fail 1 (2013) 1–20.
[2] S. Heymans, A. Gonzalez, A. Pizard, A.P. Papageorgiou, N. Lopez-Andres, F. Jaisser, et al., Searching for new mechanisms of myocardial fibrosis with diagnostic and/or therapeutic potential, Eur. J. Heart Fail. 17 (2015) 764–771.
[3] D.P. Bartel, MicroRNAs: target recognition and regulatory functions, Cell 136 (2009) 215–233.
[4] A. Ucar, S.K. Gupta, J. Fiedler, E. Erikci, M. Kardasinski, S. Batkai, et al., The miRNA-212/132 family regulates both cardiac hypertrophy and cardiomyocyte autophagy, Nat. Commun. 3 (2012) 1078.
[5] A. Foinquinos, S. Batkai, C. Genschel, J. Viereck, S. Rump, M. Gyongyosi, et al., Preclinical development of a miR-132 inhibitor for heart failure treatment, Nat Commun 11 (2020) 633, 020-14349-2.
[6] M. Brock, V.J. Samillan, M. Trenkmann, C. Schwarzwald, S. Ulrich, R.E. Gay, et al., AntagomiR directed against miR-20a restores functional BMPR2 signalling and prevents vascular remodelling in hypoxia-induced pulmonary hypertension, Eur. Heart J. 35 (2014) 3203–3211.
[7] T. Thum, C. Gross, J. Fiedler, T. Fischer, S. Kissler, M. Bussen, et al., MicroRNA-21 contributes to myocardial disease by stimulating MAP kinase signalling in fibroblasts, Nature 456 (2008) 980–984.
[8] S.K. Gupta, R. Itagaki, X. Zheng, S. Batkai, S. Thum, F. Ahmad, et al., miR-21 promotes fibrosis in an acute cardiac allograft transplantation model, Cardiovasc. Res. 110 (2016) 215–226.
[9] T. Moore-Morris, N. Guimaraes-Camboa, I. Banerjee, A.C. Zambon, T. Kisseleva, A. Velayoudon, et al., Resident fibroblast lineages mediate pressure overload-induced cardiac fibrosis, J. Clin. Invest. 124 (2014) 2921–2934.
[10] T.V. Eskildsen, P.L. Jeppesen, M. Schneider, A.Y. Nossent, M.B. Sandberg, P. B. Hansen, et al., Angiotensin II regulates microRNA-132/−212 in hypertensive rats and humans, Int. J. Mol. Sci. 14 (2013) 11190–11207.

[11] S. Shrivastava, J. Petrone, R. Steele, G.M. Lauer, A.M. Di Bisceglie, R.B. Ray, Up-regulation of circulating miR-20a is correlated with hepatitis C virus-mediated liver disease progression, Hepatology 58 (2013) 863–871.
[12] C. Doebele, A. Bonauer, A. Fischer, A. Scholz, Y. Reiss, C. Urbich, et al., Members of the microRNA-17-92 cluster exhibit a cell-intrinsic antiangiogenic function in endothelial cells, Blood 115 (2010) 4944–4950.
[13] P.A. da Costa Martins, K. Salic, M.M. Gladka, A.S. Armand, S. Leptidis, H. el Azzouzi, et al., MicroRNA-199b targets the nuclear kinase Dyrk1a in an auto-amplification loop promoting calcineurin/NFAT signalling, Nat. Cell Biol. 12 (2010) 1220–1227.
[14] R.L. Montgomery, T.G. Hullinger, H.M. Semus, B.A. Dickinson, A.G. Seto, J. M. Lynch, et al., Therapeutic inhibition of miR-208a improves cardiac function and survival during heart failure, Circulation 124 (2011) 1537–1547.
[15] A. Nakai, O. Yamaguchi, T. Takeda, Y. Higuchi, S. Hikoso, M. Taniike, et al., The role of autophagy in cardiomyocytes in the basal state and in response to hemodynamic stress, Nat. Med. 13 (2007) 619–624.
[16] P. Aranguiz-Urroz, J. Canales, M. Copaja, R. Troncoso, J.M. Vicencio, C. Carrillo, et al., Beta(2)-adrenergic receptor regulates cardiac fibroblast autophagy and collagen degradation, Biochim. Biophys. Acta 1812 (2011) 23–31.
[17] S.D. Stojanovic, M. Fuchs, J. Fiedler, K. Xiao, A. Meinecke, A. Just, et al., Comprehensive Bioinformatics Identifies Key microRNA Players in ATG7-Deficient Lung Fibroblasts, Int J Mol Sci 21 (2020), https://doi.org/10.3390/ijms21114126.
[18] P. Kong, P. Christia, N.G. Frangogiannis, The pathogenesis of cardiac fibrosis, Cell. Mol. Life Sci. 71 (2014) 549–574.
[19] D.F. Dai, L.F. Santana, M. Vermulst, D.M. Tomazela, M.J. Emond, M.J. MacCoss, et al., Overexpression of catalase targeted to mitochondria attenuates murine cardiac aging, Circulation 119 (2009) 2789–2797.
[20] G.M. Pieper, V. Nilakantan, T.K. Nguyen, G. Hilton, A.M. Roza, C.P. Johnson, Reactive oxygen and reactive nitrogen as signaling molecules for caspase 3 activation in acute cardiac transplant rejection, Antioxid. Redox Signal. 10 (2008) 1031–1040.